Supporting Information: Transferred-Rotational-Echo DOuble Resonance (TREDOR)

Xizhou Cecily Zhang,[†,‡] Marcel C. Forster,[†,‡] Evgeny Nimerovsky,[†] Kumar Tekwani Movellan,[†] and Loren B. Andreas[*,†]

†*NMR-based Structural Biology, Max-Planck-Institute for Biophysical Chemistry, Am Faßberg 11, 37077 Göttingen, Germany*

‡*Equal Contribution*

E-mail: land@nmr.mpibpc.mpg.de

Figure S1. Fitting of all contacts observed in SH3 by pseudo-4D TREDOR

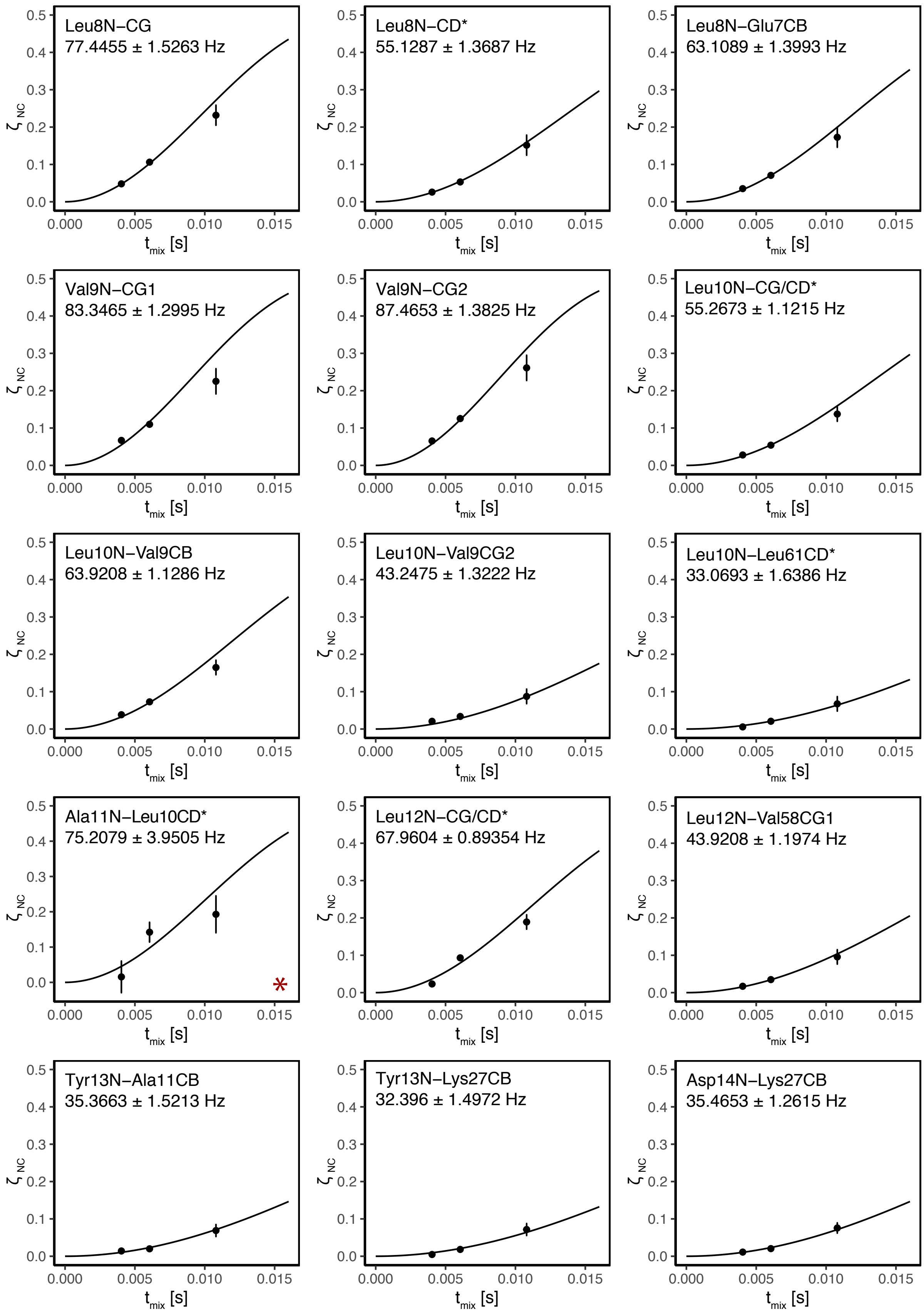

Leu8N−CG
77.4455 ± 1.5263 Hz
Leu8N−CD*
55.1287 ± 1.3687 Hz
Leu8N−Glu7CB
63.1089 ± 1.3993 Hz
Val9N−CG1
83.3465 ± 1.2995 Hz
Val9N−CG2
87.4653 ± 1.3825 Hz
Leu10N−CG/CD*
55.2673 ± 1.1215 Hz
Leu10N−Val9CB
63.9208 ± 1.1286 Hz
Leu10N−Val9CG2
43.2475 ± 1.3222 Hz
Leu10N−Leu61CD*
33.0693 ± 1.6386 Hz
Ala11N−Leu10CD*
75.2079 ± 3.9505 Hz
Leu12N−CG/CD*
67.9604 ± 0.89354 Hz
Leu12N−Val58CG1
43.9208 ± 1.1974 Hz
Tyr13N−Ala11CB
35.3663 ± 1.5213 Hz
Tyr13N−Lys27CB
32.396 ± 1.4972 Hz
Asp14N−Lys27CB
35.4653 ± 1.2615 Hz
ζ_{NC}
t_{mix} [s]

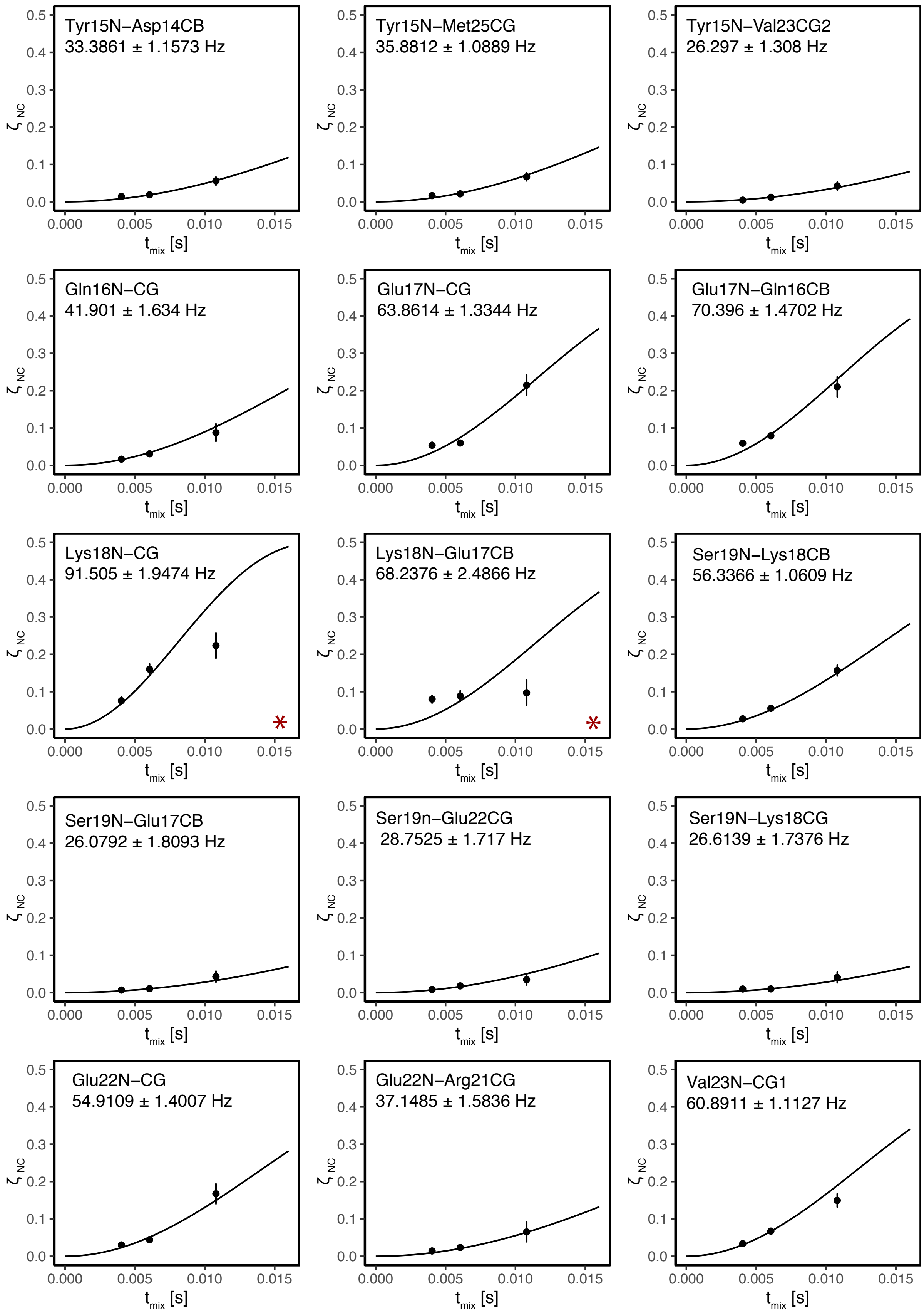
Tyr15N−Asp14CB
33.3861 ± 1.1573 Hz
Tyr15N−Met25CG
35.8812 ± 1.0889 Hz
Tyr15N−Val23CG2
26.297 ± 1.308 Hz
Gln16N−CG
41.901 ± 1.634 Hz
Glu17N−CG
63.8614 ± 1.3344 Hz
Glu17N−Gln16CB
70.396 ± 1.4702 Hz
Lys18N−CG
91.505 ± 1.9474 Hz
Lys18N−Glu17CB
68.2376 ± 2.4866 Hz
Ser19N−Lys18CB
56.3366 ± 1.0609 Hz
Ser19N−Glu17CB
26.0792 ± 1.8093 Hz
Ser19n−Glu22CG
28.7525 ± 1.717 Hz
Ser19N−Lys18CG
26.6139 ± 1.7376 Hz
Glu22N−CG
54.9109 ± 1.4007 Hz
Glu22N−Arg21CG
37.1485 ± 1.5836 Hz
Val23N−CG1
60.8911 ± 1.1127 Hz
ζ NC
t mix [s]
0.0 0.1 0.2 0.3 0.4 0.5
0.000 0.005 0.010 0.015

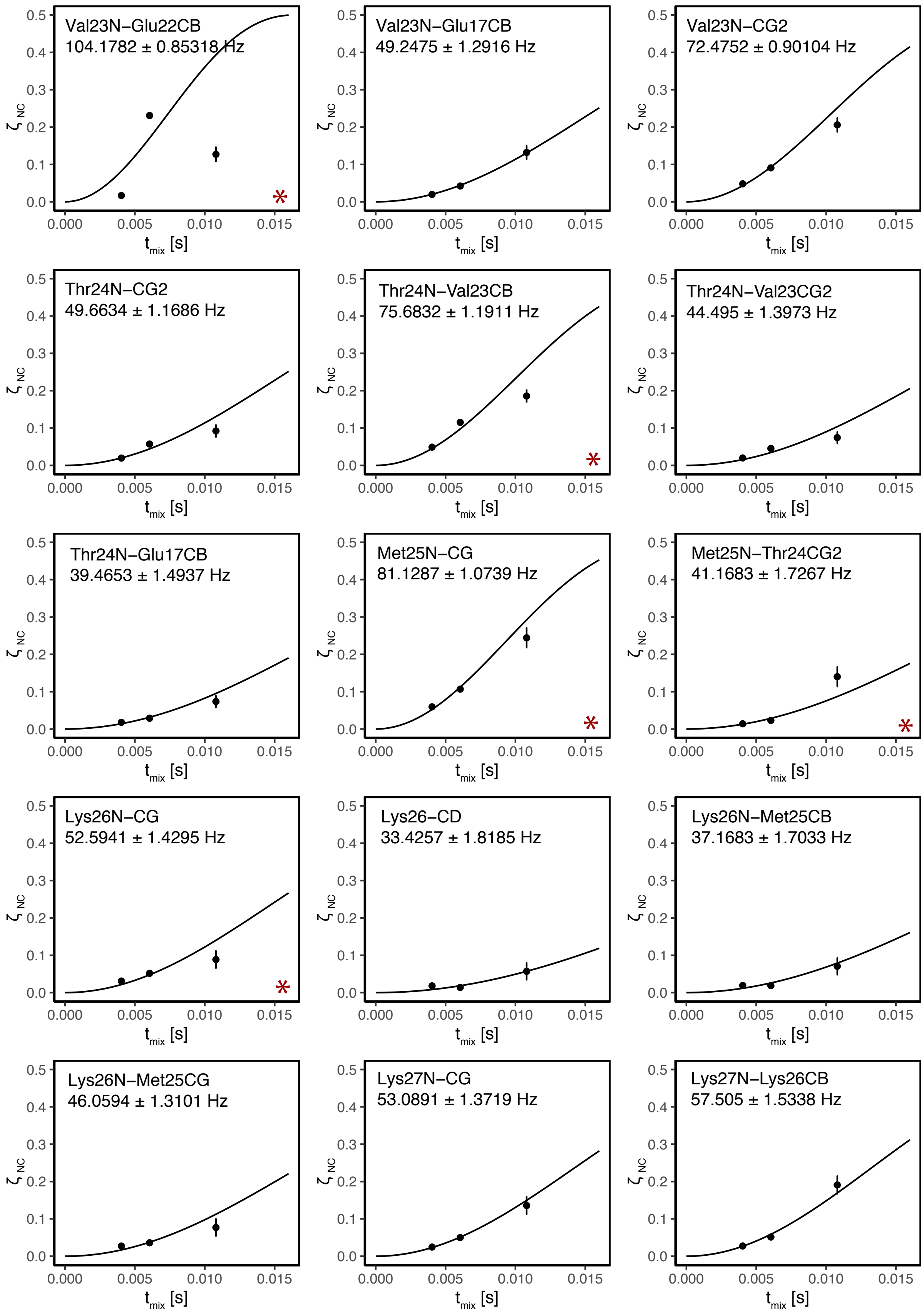
Val23N–Glu22CB
104.1782 ± 0.85318 Hz
Val23N–Glu17CB
49.2475 ± 1.2916 Hz
Val23N–CG2
72.4752 ± 0.90104 Hz
Thr24N–CG2
49.6634 ± 1.1686 Hz
Thr24N–Val23CB
75.6832 ± 1.1911 Hz
Thr24N–Val23CG2
44.495 ± 1.3973 Hz
Thr24N–Glu17CB
39.4653 ± 1.4937 Hz
Met25N–CG
81.1287 ± 1.0739 Hz
Met25N–Thr24CG2
41.1683 ± 1.7267 Hz
Lys26N–CG
52.5941 ± 1.4295 Hz
Lys26–CD
33.4257 ± 1.8185 Hz
Lys26N–Met25CB
37.1683 ± 1.7033 Hz
Lys26N–Met25CG
46.0594 ± 1.3101 Hz
Lys27N–CG
53.0891 ± 1.3719 Hz
Lys27N–Lys26CB
57.505 ± 1.5338 Hz
ζ NC
t mix [s]

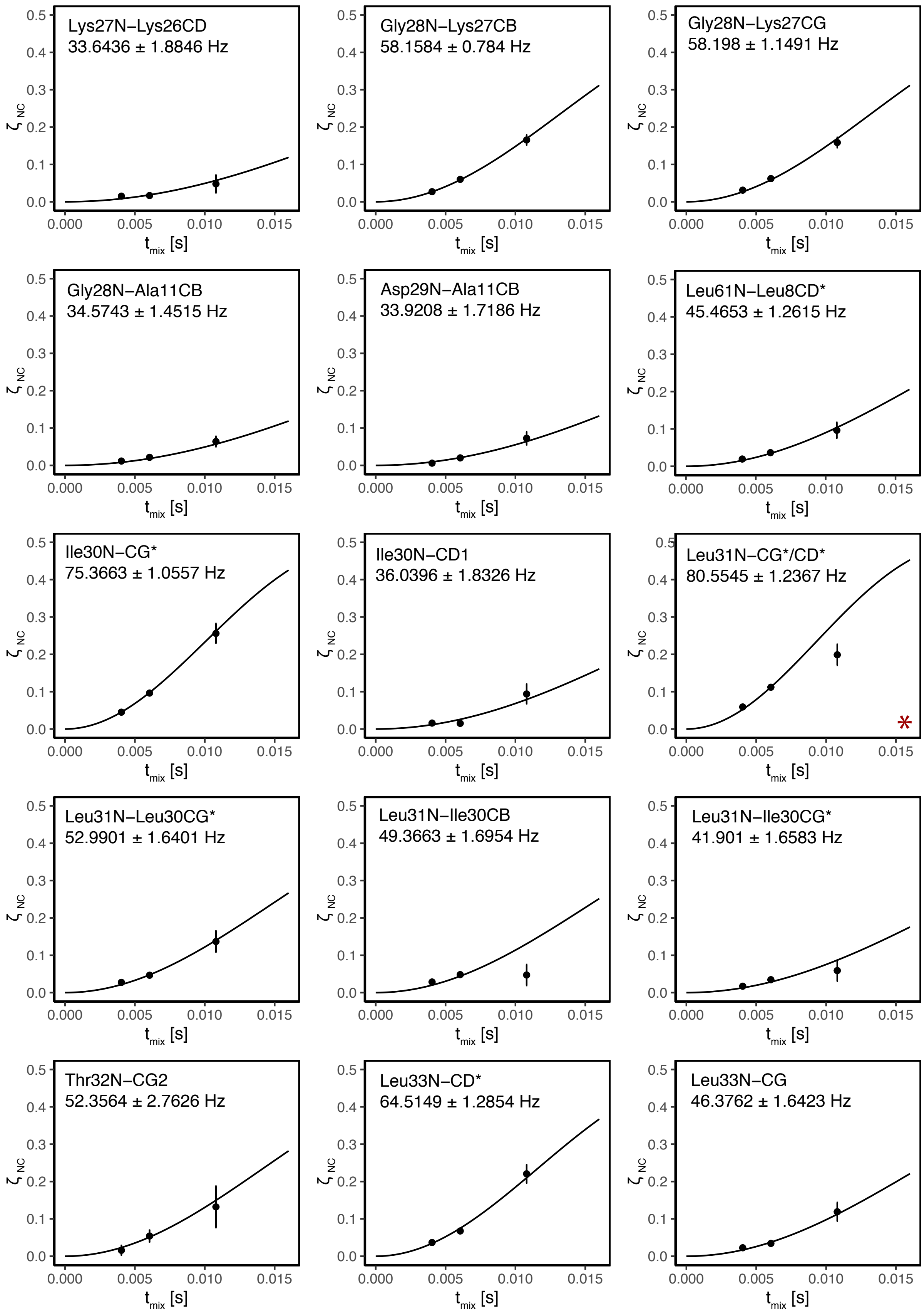

Lys27N–Lys26CD
33.6436 ± 1.8846 Hz
Gly28N–Lys27CB
58.1584 ± 0.784 Hz
Gly28N–Lys27CG
58.198 ± 1.1491 Hz
Gly28N–Ala11CB
34.5743 ± 1.4515 Hz
Asp29N–Ala11CB
33.9208 ± 1.7186 Hz
Leu61N–Leu8CD*
45.4653 ± 1.2615 Hz
Ile30N–CG*
75.3663 ± 1.0557 Hz
Ile30N–CD1
36.0396 ± 1.8326 Hz
Leu31N–CG*/CD*
80.5545 ± 1.2367 Hz
Leu31N–Leu30CG*
52.9901 ± 1.6401 Hz
Leu31N–Ile30CB
49.3663 ± 1.6954 Hz
Leu31N–Ile30CG*
41.901 ± 1.6583 Hz
Thr32N–CG2
52.3564 ± 2.7626 Hz
Leu33N–CD*
64.5149 ± 1.2854 Hz
Leu33N–CG
46.3762 ± 1.6423 Hz
ζ_{NC}
t_{mix} [s]

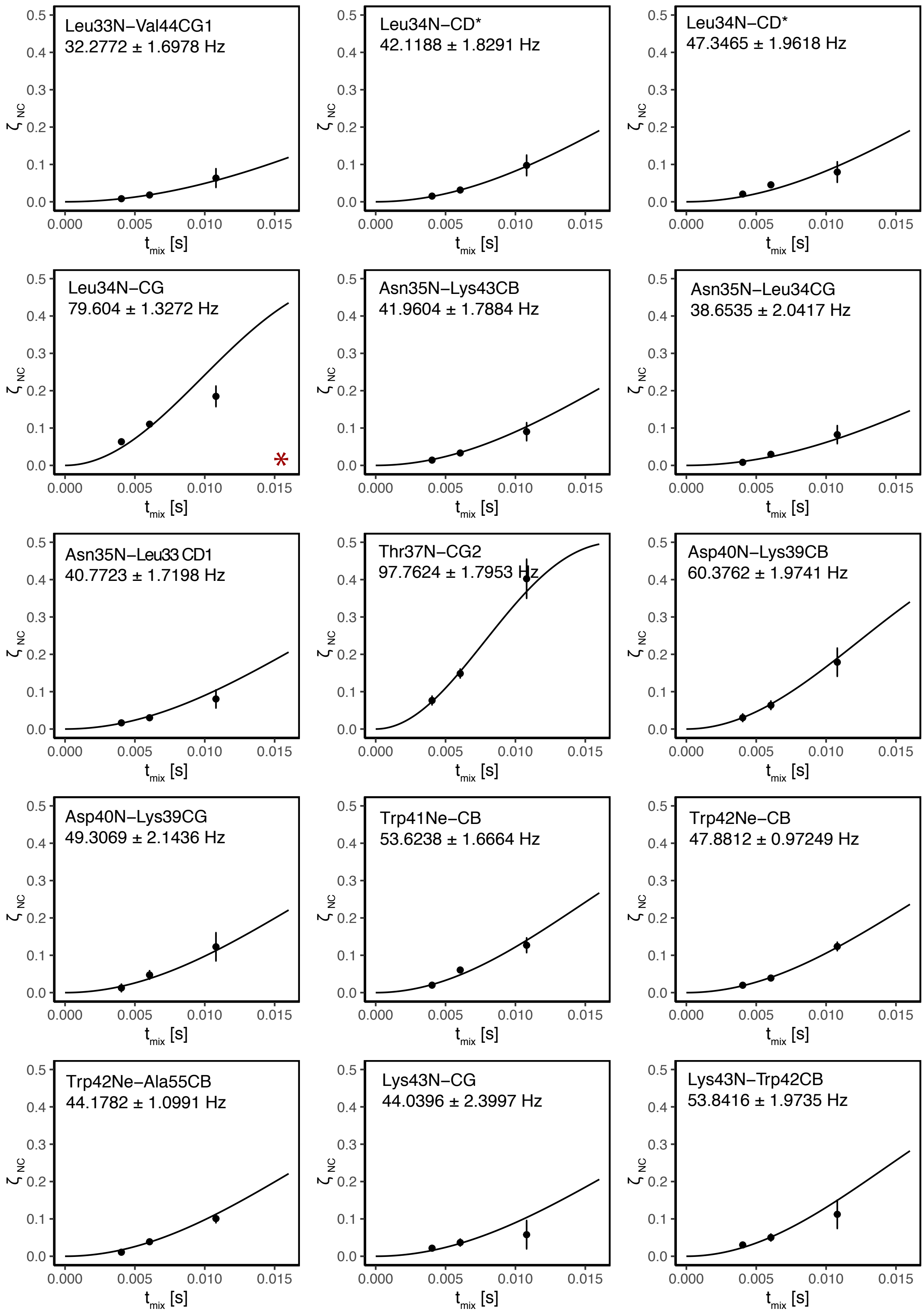
Leu33N−Val44CG1
32.2772 ± 1.6978 Hz
Leu34N−CD*
42.1188 ± 1.8291 Hz
Leu34N−CD*
47.3465 ± 1.9618 Hz
Leu34N−CG
79.604 ± 1.3272 Hz
Asn35N−Lys43CB
41.9604 ± 1.7884 Hz
Asn35N−Leu34CG
38.6535 ± 2.0417 Hz
Asn35N−Leu33 CD1
40.7723 ± 1.7198 Hz
Thr37N−CG2
97.7624 ± 1.7953 Hz
Asp40N−Lys39CB
60.3762 ± 1.9741 Hz
Asp40N−Lys39CG
49.3069 ± 2.1436 Hz
Trp41Ne−CB
53.6238 ± 1.6664 Hz
Trp42Ne−CB
47.8812 ± 0.97249 Hz
Trp42Ne−Ala55CB
44.1782 ± 1.0991 Hz
Lys43N−CG
44.0396 ± 2.3997 Hz
Lys43N−Trp42CB
53.8416 ± 1.9735 Hz
ζ NC
t mix [s]

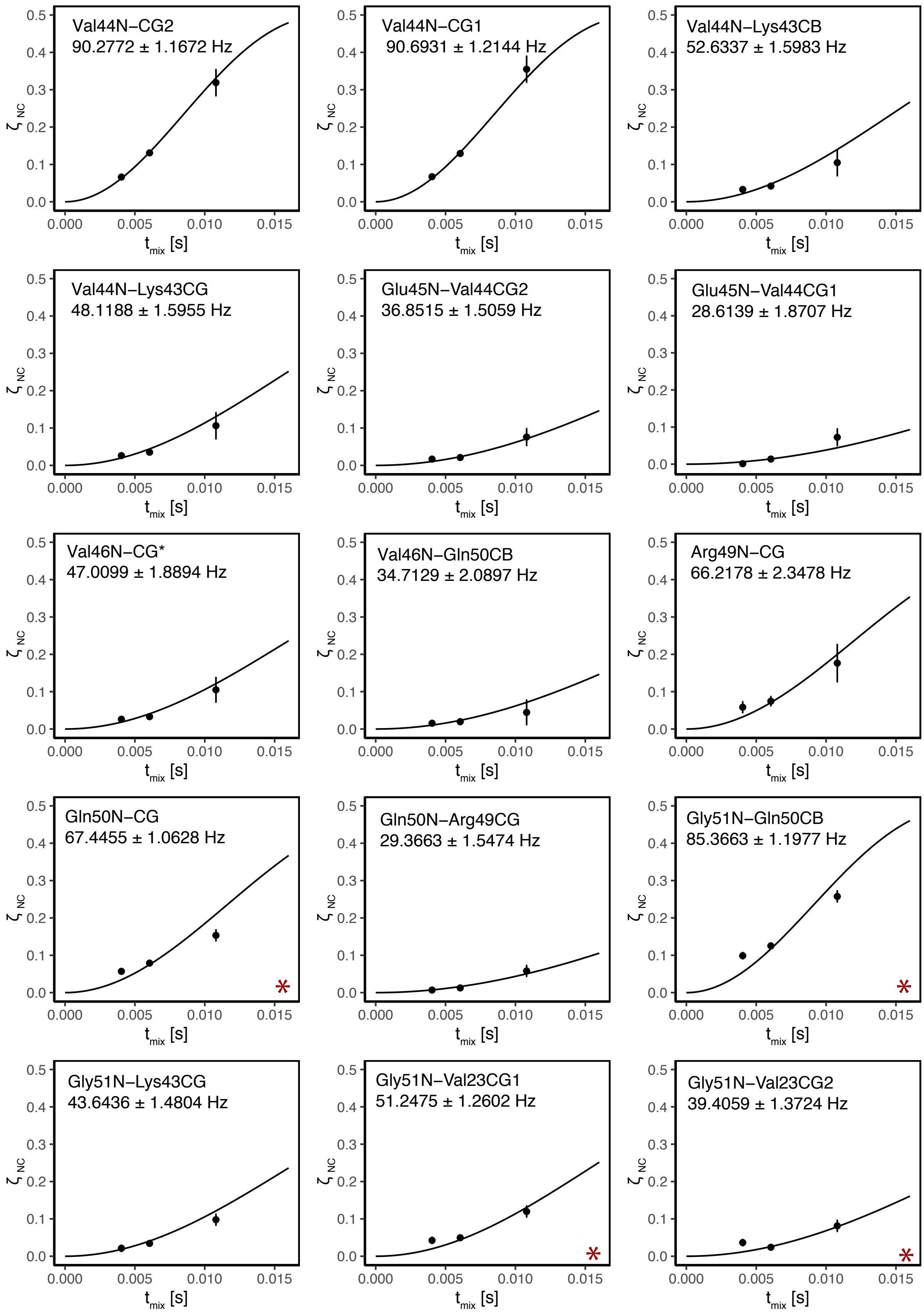
Val44N–CG2
90.2772 ± 1.1672 Hz
Val44N–CG1
90.6931 ± 1.2144 Hz
Val44N–Lys43CB
52.6337 ± 1.5983 Hz
Val44N–Lys43CG
48.1188 ± 1.5955 Hz
Glu45N–Val44CG2
36.8515 ± 1.5059 Hz
Glu45N–Val44CG1
28.6139 ± 1.8707 Hz
Val46N–CG*
47.0099 ± 1.8894 Hz
Val46N–Gln50CB
34.7129 ± 2.0897 Hz
Arg49N–CG
66.2178 ± 2.3478 Hz
Gln50N–CG
67.4455 ± 1.0628 Hz
Gln50N–Arg49CG
29.3663 ± 1.5474 Hz
Gly51N–Gln50CB
85.3663 ± 1.1977 Hz
Gly51N–Lys43CG
43.6436 ± 1.4804 Hz
Gly51N–Val23CG1
51.2475 ± 1.2602 Hz
Gly51N–Val23CG2
39.4059 ± 1.3724 Hz
ζ NC
t mix [s]

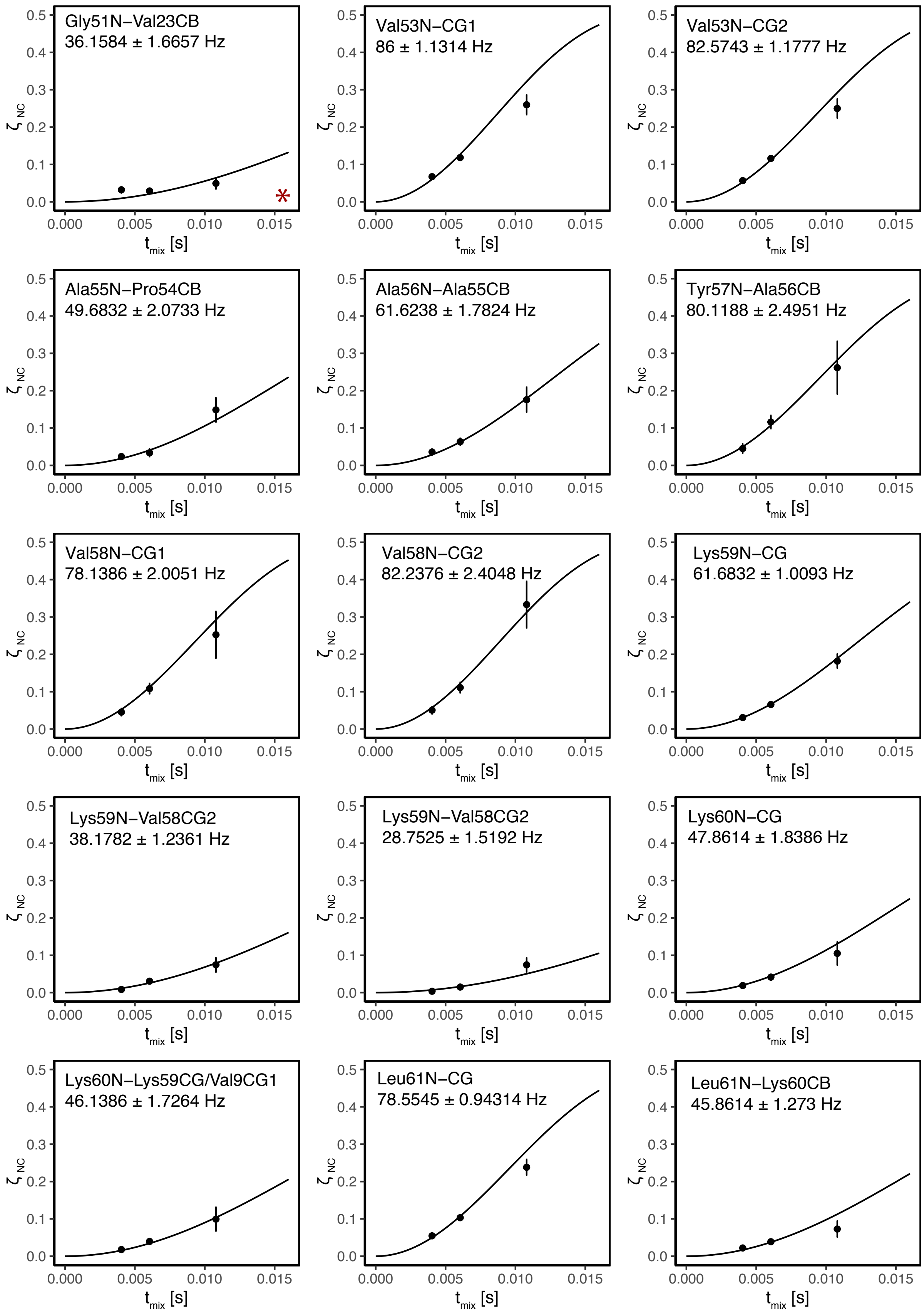
Gly51N–Val23CB
36.1584 ± 1.6657 Hz
Val53N–CG1
86 ± 1.1314 Hz
Val53N–CG2
82.5743 ± 1.1777 Hz
Ala55N–Pro54CB
49.6832 ± 2.0733 Hz
Ala56N–Ala55CB
61.6238 ± 1.7824 Hz
Tyr57N–Ala56CB
80.1188 ± 2.4951 Hz
Val58N–CG1
78.1386 ± 2.0051 Hz
Val58N–CG2
82.2376 ± 2.4048 Hz
Lys59N–CG
61.6832 ± 1.0093 Hz
Lys59N–Val58CG2
38.1782 ± 1.2361 Hz
Lys59N–Val58CG2
28.7525 ± 1.5192 Hz
Lys60N–CG
47.8614 ± 1.8386 Hz
Lys60N–Lys59CG/Val9CG1
46.1386 ± 1.7264 Hz
Leu61N–CG
78.5545 ± 0.94314 Hz
Leu61N–Lys60CB
45.8614 ± 1.273 Hz
ζ NC
t mix [s]

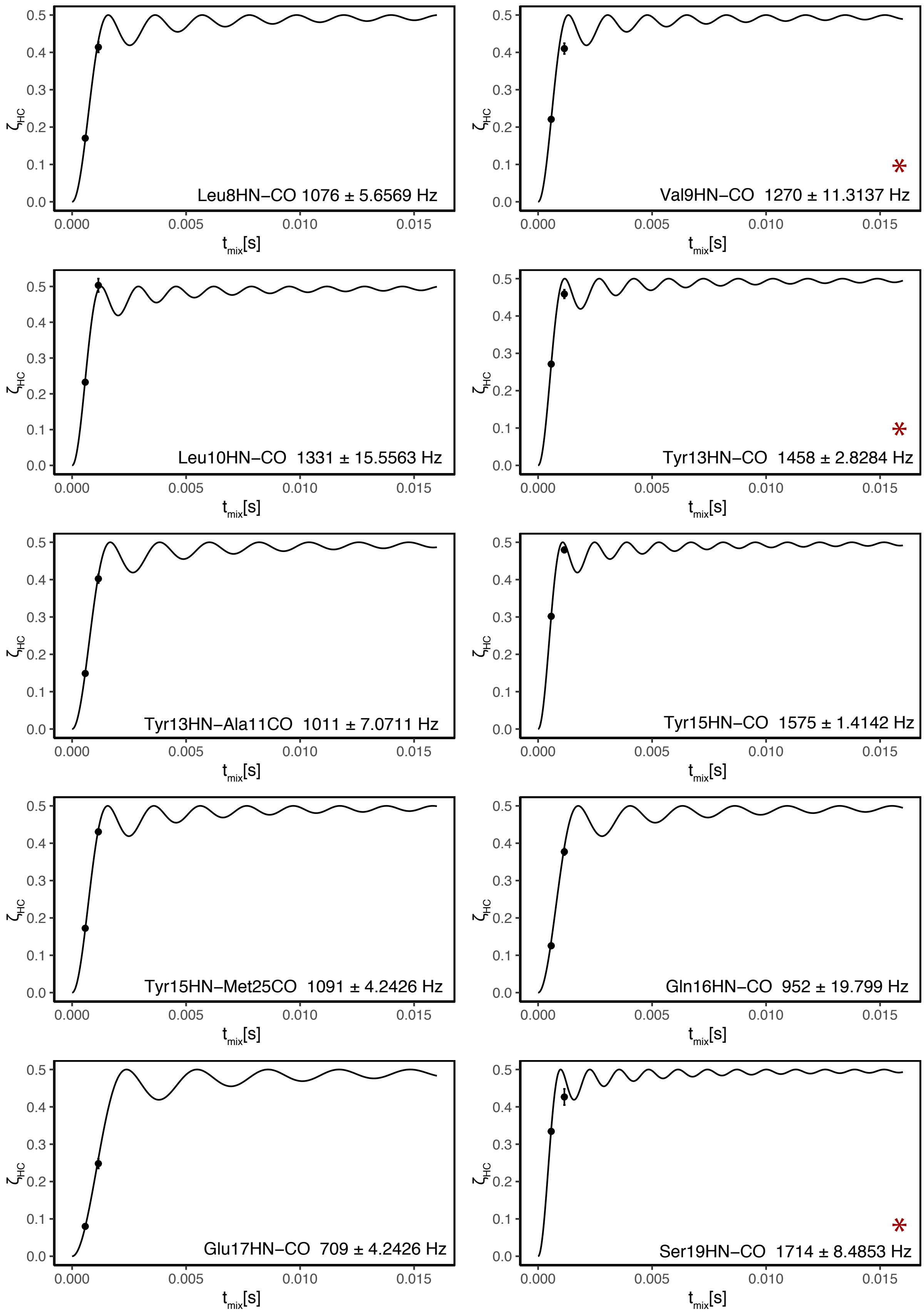
Leu8HN−CO 1076 ± 5.6569 Hz
Val9HN−CO 1270 ± 11.3137 Hz
Leu10HN−CO 1331 ± 15.5563 Hz
Tyr13HN−CO 1458 ± 2.8284 Hz
Tyr13HN−Ala11CO 1011 ± 7.0711 Hz
Tyr15HN−CO 1575 ± 1.4142 Hz
Tyr15HN−Met25CO 1091 ± 4.2426 Hz
Gln16HN−CO 952 ± 19.799 Hz
Glu17HN−CO 709 ± 4.2426 Hz
Ser19HN−CO 1714 ± 8.4853 Hz
ζ_{HC}
t_{mix}[s]
0.0
0.1
0.2
0.3
0.4
0.5
0.000
0.005
0.010
0.015
*

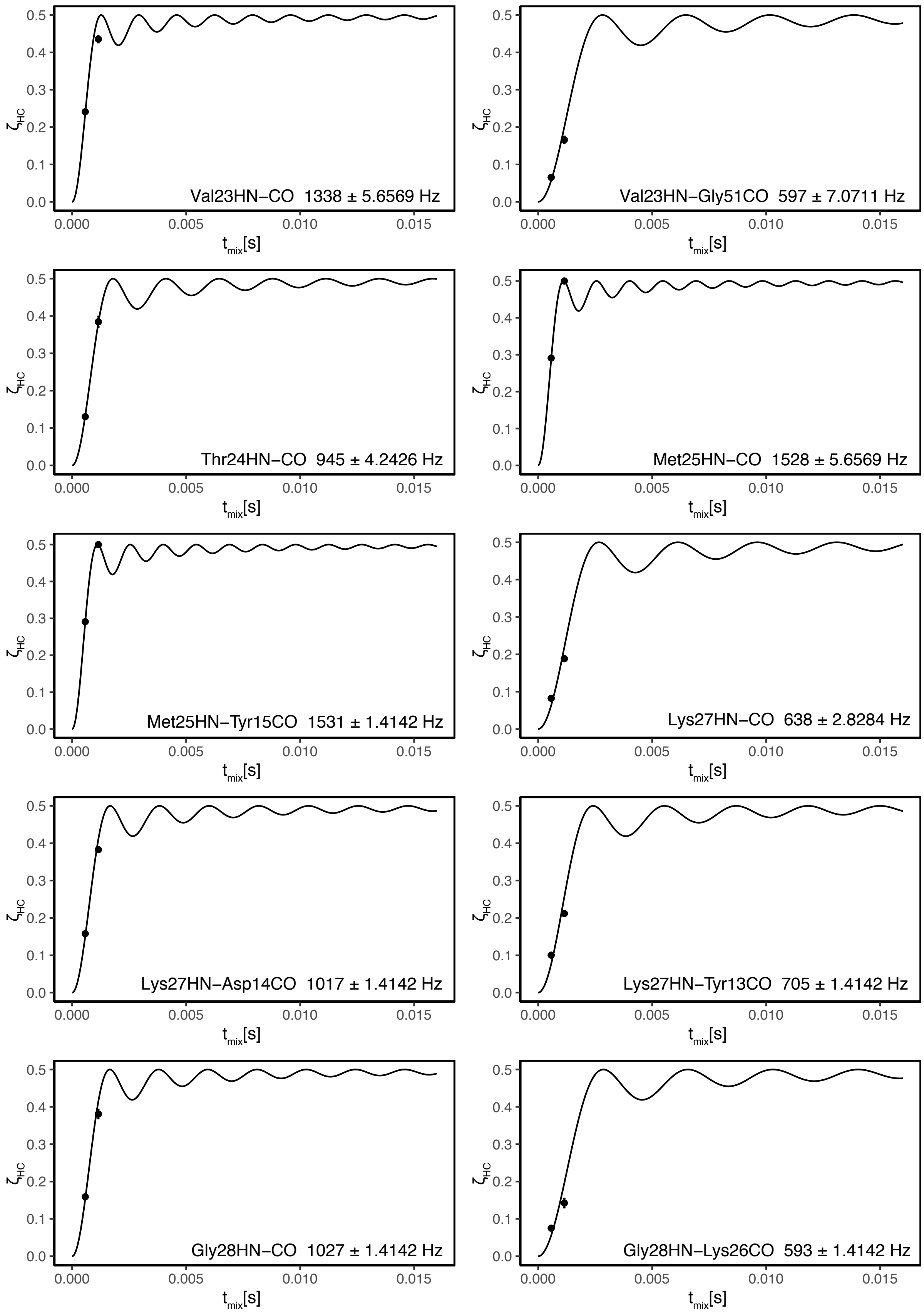
Val23HN−CO 1338 ± 5.6569 Hz
Val23HN−Gly51CO 597 ± 7.0711 Hz
Thr24HN−CO 945 ± 4.2426 Hz
Met25HN−CO 1528 ± 5.6569 Hz
Met25HN−Tyr15CO 1531 ± 1.4142 Hz
Lys27HN−CO 638 ± 2.8284 Hz
Lys27HN−Asp14CO 1017 ± 1.4142 Hz
Lys27HN−Tyr13CO 705 ± 1.4142 Hz
Gly28HN−CO 1027 ± 1.4142 Hz
Gly28HN−Lys26CO 593 ± 1.4142 Hz
ζ_{HC}
t_{mix}[s]

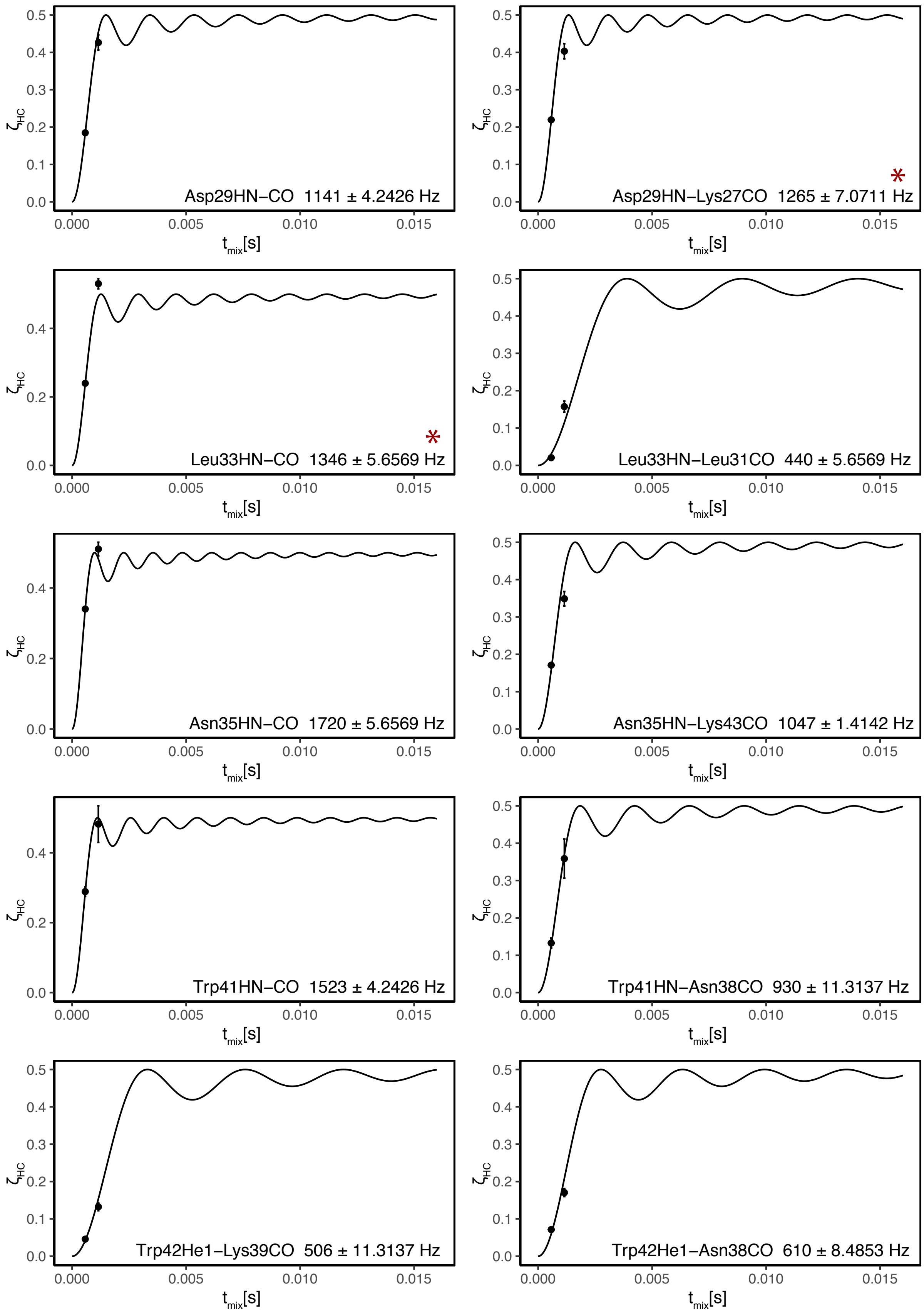

Asp29HN−CO 1141 ± 4.2426 Hz
Asp29HN−Lys27CO 1265 ± 7.0711 Hz
Leu33HN−CO 1346 ± 5.6569 Hz
Leu33HN−Leu31CO 440 ± 5.6569 Hz
Asn35HN−CO 1720 ± 5.6569 Hz
Asn35HN−Lys43CO 1047 ± 1.4142 Hz
Trp41HN−CO 1523 ± 4.2426 Hz
Trp41HN−Asn38CO 930 ± 11.3137 Hz
Trp42He1−Lys39CO 506 ± 11.3137 Hz
Trp42He1−Asn38CO 610 ± 8.4853 Hz
ζHC
tmix[s]

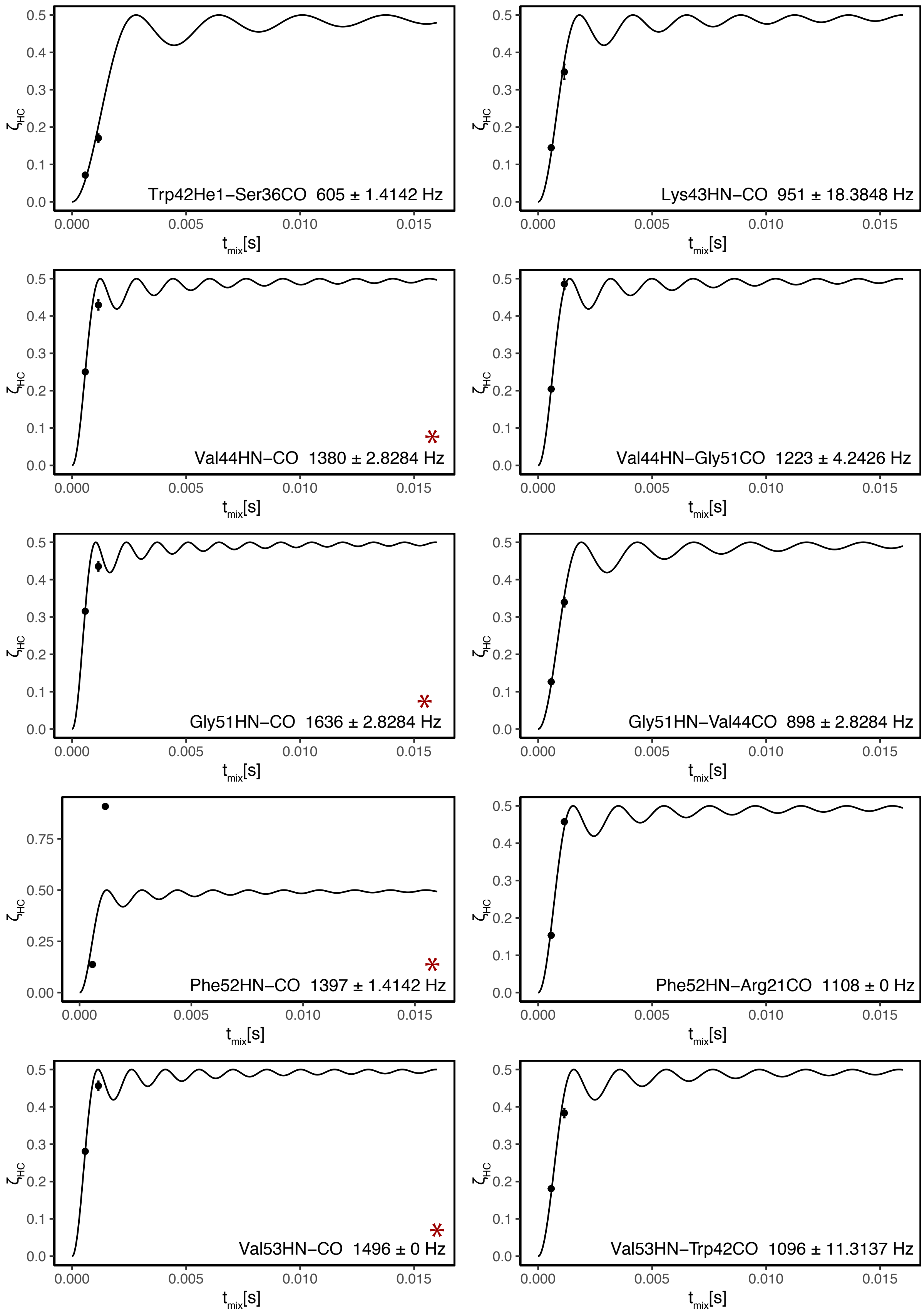
ζHC
tmix[s]
Trp42He1−Ser36CO 605 ± 1.4142 Hz
Lys43HN−CO 951 ± 18.3848 Hz
Val44HN−CO 1380 ± 2.8284 Hz
Val44HN−Gly51CO 1223 ± 4.2426 Hz
Gly51HN−CO 1636 ± 2.8284 Hz
Gly51HN−Val44CO 898 ± 2.8284 Hz
Phe52HN−CO 1397 ± 1.4142 Hz
Phe52HN−Arg21CO 1108 ± 0 Hz
Val53HN−CO 1496 ± 0 Hz
Val53HN−Trp42CO 1096 ± 11.3137 Hz
*

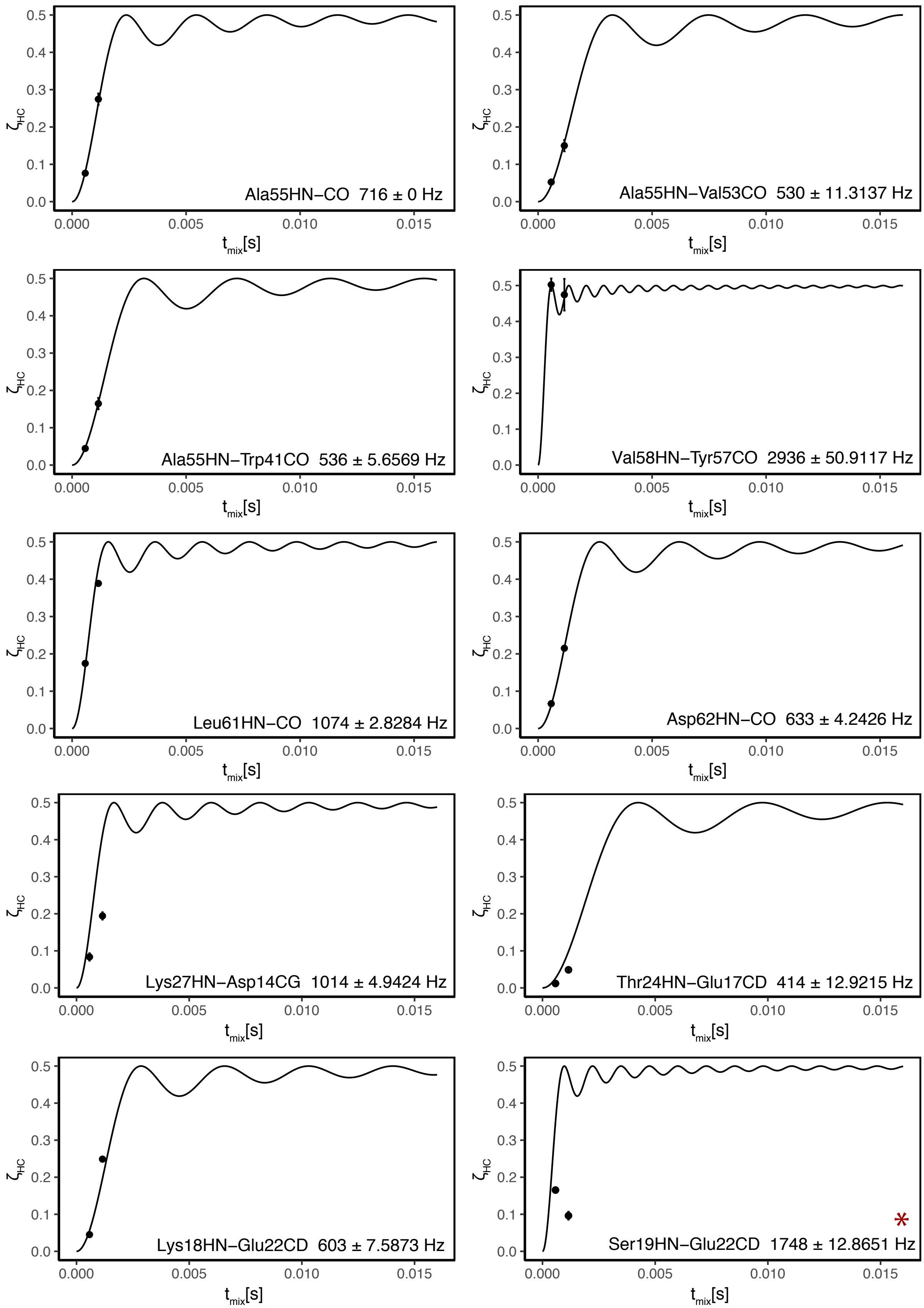
Ala55HN−CO 716 ± 0 Hz
Ala55HN−Val53CO 530 ± 11.3137 Hz
Ala55HN−Trp41CO 536 ± 5.6569 Hz
Val58HN−Tyr57CO 2936 ± 50.9117 Hz
Leu61HN−CO 1074 ± 2.8284 Hz
Asp62HN−CO 633 ± 4.2426 Hz
Lys27HN−Asp14CG 1014 ± 4.9424 Hz
Thr24HN−Glu17CD 414 ± 12.9215 Hz
Lys18HN−Glu22CD 603 ± 7.5873 Hz
Ser19HN−Glu22CD 1748 ± 12.8651 Hz
ζ_{HC}
t_{mix}[s]

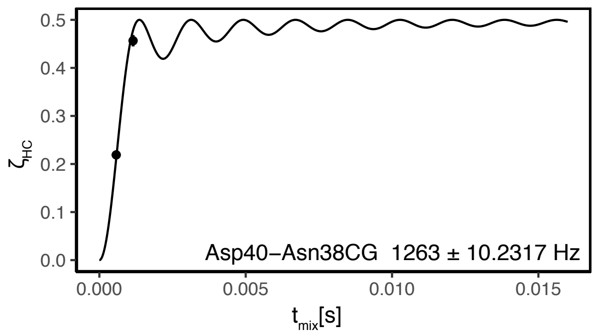

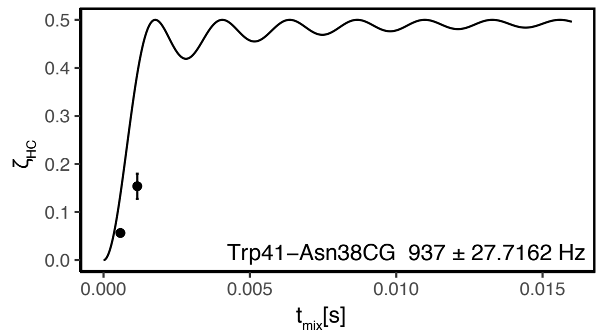

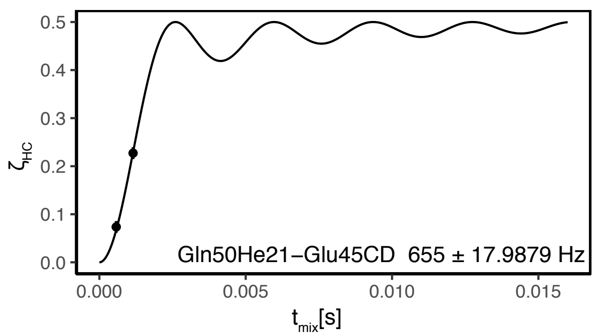

* indicates potentially compromised fit quality due to spectral overlap

Table S1. Relaxation rate Nitrogen T2 from hNH vs TREDOR relxation rate

Residue	hNH t2 [ms]	TREDOR T2[ms]	Residue	hNH t2[ms]	TREDOR T2 [ms]
7GluN	19.55	3.87	34LeuN	64.94	4.34
8LeuN	68.45	4.51	35AsnN	56.15	4.02
9ValN	67.61	3.52	37ThrN	70.08	5.82
10LeuN	64.02	4.68	38AsnN	69.74	4.46
11AlaN	103.95	0.91	39LysN	92.85	4.16
12LeuN	78.37	3.98	40AspN	49.85	5.12
13TyrN	84.67	4.93	41TrpN	64.31	3.27
14AspN	109.89	4.79	41TrpNe1	53.30	4.73
15TyrN	74.18	5.17	42TrpN	72.10	9.68
16GlnN	136.61	5.30	42TrpNe1	162.07	5.81
17GluN	88.34	5.72	43LysN	86.43	4.08
18LysN	83.61	4.42	44ValN	76.05	3.05
19SerN	65.40	5.72	45GluN	79.11	5.30
22GluN	74.35	3.57	49ArgN	52.88	6.50
23ValN	101.01	4.03	50GlnN	75.24	5.29
24ThrN	118.62	4.86	51GlyN	69.54	9.48
25MetN	79.74	3.90	52PheN	104.60	4.98
26LysN	108.70	4.21	53ValN	77.04	3.50
27LysN	106.27	3.73	55AlaN	93.37	4.64
28GlyN	70.32	6.40	56AlaN	73.42	4.73
29AspN	75.13	5.23	57TyrN	85.84	3.94
30IleN	91.49	3.59	58ValN	86.13	3.35
31LeuN	70.18	3.87	59LysN	60.28	3.14
32ThrN	90.33	4.92	60LysN	119.19	3.64
33LeuN	98.91	4.46	61LeuN	85.76	3.88

Table S2. Upper and lower distance restraints used in the structure calculation. Ambiguous restraints are given in the CYANA format as putting them with 0 Å.

Contact		Upper limit [Å]	Lower limit [Å]
8 LEU N	8 LEU CG	3.44	2.82
8 LEU N	8 LEU CD1	3.91	3.2
8 LEU N	8 LEU CD2	0	0
8 LEU N	7 GLU CB	3.78	3.09
9 VAL N	9 VAL CG1	3.44	2.81
9 VAL N	9 VAL CG2	3.31	2.71
10 LEU N	10 LEU CG	3.92	3.21
10 LEU N	10 LEU CD1	0	0
10 LEU N	10 LEU CD2	0	0
10 LEU N	9 VAL CB	3.77	3.09
10 LEU N	9 VAL CG2	4.3	3.52
10 LEU N	61 LEU CD1	4.73	3.87
10 LEU N	61 LEU CD2	0	0
11 ALA N	10 LEU CD1	3.51	2.87
11 ALA N	10 LEU CD2	0	0
12 LEU N	12 LEU CG	3.6	2.94
12 LEU N	12 LEU CD1	0	0
12 LEU N	12 LEU CD2	0	0
12 LEU N	58 VAL CG1	4.28	3.51
13 TYR N	11 ALA CB	4.54	3.71
13 TYR N	27 LYS CB	4.77	3.9
14 ASP N	27 LYS CB	4.53	3.7
15 TYR N	14 ASP CB	4.77	3.24
15 TYR N	25 MET CG	4.45	3.64
15 TYR N	25 MET CE	5.05	4.01
16 GLN N	16 GLN CG	4.33	3.54
17 GLU N	17 GLU CG	3.76	3.08
17 GLU N	16 GLN CB	3.6	2.94
18 LYS N	18 LYS CG	3.3	2.7
18 LYS N	17 GLU CB	3.62	2.96
19 SER N	18 LYS CB	3.82	3.12
19 SER N	17 GLU CB	4.93	4.03
19 SER N	22 GLU CG	4.78	3.91
19 SER N	18 LYS CG	4.97	4.07
22 GLU N	22 GLU CG	3.91	3.2
22 GLU N	21 ARG CG	4.39	3.59
23 VAL N	23 VAL CG1	3.79	3.1
23 VAL N	22 GLU CB	3.18	2.6
23 VAL N	17 GLU CB	4.03	3.29
23 VAL N	23 VAL CG2	3.6	2.94
24 THR N	24 THR CG2	4.03	3.29
24 THR N	23 VAL CB	3.49	2.86
24 THR N	23 VAL CG2	4.23	3.46

24 THR N	17 GLU CB	4.34	3.55
25 MET N	25 MET CG	3.44	2.82
25 MET N	24 THR CG2	4.34	3.55
26 LYS N	26 LYS CG	4.02	3.29
26 LYS N	26 LYS CD	4.7	3.85
26 LYS N	25 MET CB	4.4	3.6
26 LYS N	25 MET CG	4.09	3.35
27 LYS N	27 LYS CG	4.02	3.29
27 LYS N	26 LYS CB	3.79	3.1
27 LYS N	26 LYS CD	4.69	3.83
28 GLY N	27 LYS CB	3.79	3.1
28 GLY N	27 LYS CG	3.79	3.1
28 GLY N	11 ALA CB	4.59	3.75
29 ASP N	11 ALA CB	4.7	3.85
30 ILE N	30 ILE CG1	3.49	2.86
30 ILE N	30 ILE CD1	4.5	3.68
31 LEU N	30 ILE CG1	4.03	3.29
31 LEU N	30 ILE CB	4.32	3.58
32 THR N	32 THR CG2	3.98	3.26
33 LEU N	33 LEU CD1	3.73	3.05
33 LEU N	33 LEU CD2	0	0
33 LEU N	33 LEU CG	4.07	3.33
33 LEU N	44 VAL CG1	4.75	3.88
34 LEU N	34 LEU CD1	4.31	3.52
34 LEU N	34 LEU CD2	0	0
34 LEU N	34 LEU CD1	4.06	3.32
34 LEU N	34 LEU CD2	0	0
34 LEU N	34 LEU CG	3.44	2.82
35 ASN N	43 LYS CB	4.32	3.53
35 ASN N	34 LEU CG	4.35	3.56
35 ASN N	33 LEU CD1	4.33	3.54
37 THR N	37 THR CG2	3.2	2.62
40 ASP N	39 LYS CB	3.78	3.1
40 ASP N	39 LYS CG	4.05	3.31
43 LYS N	43 LYS CG	4.2	3.44
43 LYS N	42 TRP CB	3.96	3.24
44 VAL N	44 VAL CG2	3.31	2.71
44 VAL N	44 VAL CG1	3.31	2.71
44 VAL N	43 LYS CB	4.02	3.29
44 VAL N	43 LYS CG	4.03	3.3
45 GLU N	44 VAL CG2	4.38	3.59
45 GLU N	44 VAL CG1	4.8	3.93
46 VAL N	46 VAL CG1	4.07	3.33
46 VAL N	50 GLN CB	4.56	3.73
49 ARG N	49 ARG CG	3.64	2.98
50 GLN N	50 GLN CG	3.6	2.95
50 GLN N	49 ARG CG	4.77	3.91

51 GLY N	50 GLN CB	3.36	2.75
51 GLY N	43 LYS CG	4.28	3.51
51 GLY N	23 VAL CG1	4.03	3.29
51 GLY N	23 VAL CG2	4.34	3.55
51 GLY N	23 VAL CB	4.46	3.65
53 VAL N	53 VAL CG1	3.33	2.73
53 VAL N	53 VAL CG2	3.44	2.81
55 ALA N	54 PRO CB	4.03	3.3
56 ALA N	55 ALA CB	3.79	3.1
57 TYR N	56 ALA CB	3.44	2.81
58 VAL N	58 VAL CG1	3.45	2.83
58 VAL N	58 VAL CG2	3.44	2.81
59 LYS N	59 LYS CG	3.79	3.1
59 LYS N	58 VAL CG2	4.34	3.55
59 LYS N	58 VAL CG1	4.78	3.91
60 LYS N	60 LYS CG	4.07	3.33
60 LYS N	59 LYS CG	4.11	3.36
60 LYS N	9 VAL CG1	4.11	3.36
61 LEU N	61 LEU CG	3.44	2.82
61 LEU N	60 LYS CB	4.09	3.34
61 LEU N	61 LEU CD1	4.16	3.4
61 LEU N	61 LEU CD2	0	0
41 TRP NE1	41 TRP CB	3.98	3.26
42 TRP NE1	42 TRP CB	4.03	3.29
42 TRP NE1	55 ALA CB	4.29	3.51
31 LEU N	31 LEU CD2	3.44	2.82
31 LEU N	31 LEU CG	4	3.27
31 LEU N	31 LEU CD1	0	0
31 LEU N	31 LEU CD2	0	0
8 LEU H	8 LEU C	3.1	2.54
9 VAL H	9 VAL C	2.95	2.41
10 LEU H	10 LEU C	2.89	2.37
13 TYR H	13 TYR C	2.81	2.3
13 TYR H	11 ALA C	3.17	2.59
15 TYR H	15 TYR C	2.73	2.23
15 TYR H	25 MET C	3.09	2.53
16 GLN H	16 GLN C	2.65	2.17
17 GLU H	17 GLU C	3.56	2.92
19 SER H	19 SER C	2.66	2.18
23 VAL H	23 VAL C	2.88	2.36
23 VAL H	51 GLY C	3.8	3.11
24 THR H	24 THR C	3.25	2.66
25 MET H	25 MET C	2.76	2.26
25 MET H	15 TYR C	2.76	2.26
27 LYS H	27 LYS C	3.69	3.02
27 LYS H	14 ASP C	3.17	3.17
27 LYS H	13 TYR C	3.56	2.92

28 GLY H	28 GLY C	3.15	2.57
28 GLY H	26 LYS C	3.78	3.1
29 ASP H	29 ASP C	3.04	2.48
29 ASP H	27 LYS C	2.95	2.41
33 LEU H	33 LEU C	2.88	2.36
33 LEU H	31 LEU C	4.2	3.44
35 ASN H	35 ASN C	2.65	2.17
35 ASN H	43 LYS C	3.14	2.57
41 TRP H	41 TRP C	2.75	2.25
41 TRP H	38 ASN C	3.25	2.66
42 TRP H	53 VAL C	3.05	2.49
42 TRP HE1	39 LYS C	4	3.28
42 TRP HE1	38 ASN C	3.76	3.08
42 TRP HE1	36 SER C	3.76	3.08
43 LYS H	43 LYS C	3.22	2.64
44 VAL H	44 VAL C	2.86	2.34
44 VAL H	51 GLY C	2.98	2.44
51 GLY H	51 GLY C	2.7	2.21
51 GLY H	44 VAL C	3.3	2.7
52 PHE H	52 PHE C	2.84	2.32
52 PHE H	21 ARG C	3.07	2.51
53 VAL H	53 VAL C	2.78	2.28
53 VAL H	42 TRP C	3.08	2.52
55 ALA H	55 ALA C	3.54	2.9
55 ALA H	53 VAL C	3.89	3.19
55 ALA H	41 TRP C	3.93	3.21
58 VAL H	58 VAL C	2.89	2.37
61 LEU H	61 LEU C	3.1	2.54
62 ASP H	62 ASP C	3.7	3.02
27 LYS H	14 ASP CG	3.17	2.59
24 THR H	17 GLU CD	4.27	3.49
18 LYS H	22 GLU CD	3.77	3.08
19 SER H	22 GLU CD	2.64	2.16
40 ASP H	38 ASN CG	2.94	2.41
41 TRP H	38 ASN CG	3.25	2.66
50 GLN HE21	45 GLU CD	3.45	2.82

Table S3. TALOS-N angle restraints.

Residue		Angle	Angle margin	
8	LEU	PHI	-155.7	-108
8	LEU	PSI	135.2	175.2
9	VAL	PHI	-148.2	-108.2
9	VAL	PSI	131.4	171.4
10	LEU	PHI	-145.1	-105.1
10	LEU	PSI	116.5	156.5
11	ALA	PHI	-94.3	-52.8
11	ALA	PSI	106.7	146.7
12	LEU	PHI	-103.9	-63.1
12	LEU	PSI	-60.8	-19.7
13	TYR	PHI	-182.5	-131.4
13	TYR	PSI	138	178
16	GLN	PHI	-149.5	-86.9
16	GLN	PSI	109.4	169.9
23	VAL	PHI	-175.6	-72.5
23	VAL	PSI	129.5	177.3
24	THR	PHI	-132.1	-83.3
24	THR	PSI	111.5	151.5
25	MET	PHI	-151.5	-89.7
25	MET	PSI	113.5	171.6
26	LYS	PHI	-118	-56.7
26	LYS	PSI	130.5	170.5
27	LYS	PHI	-76.5	-36.5
27	LYS	PSI	113.2	153.2
29	ASP	PHI	-84.6	-44.6
29	ASP	PSI	126.3	166.3
30	ILE	PHI	-129.2	-89.2
30	ILE	PSI	104.5	144.5
31	LEU	PHI	-130	-89.1
31	LEU	PSI	103.8	158.4
32	THR	PHI	-97.3	-52.6
32	THR	PSI	107.9	147.9
33	LEU	PHI	-117.8	-50.3
33	LEU	PSI	88.7	168.2
34	LEU	PHI	-79.4	-39.4
34	LEU	PSI	-51.9	-11.9
36	SER	PHI	-88.8	-48.8
36	SER	PSI	-55.9	-15.9
37	THR	PHI	-85.9	-45.9
37	THR	PSI	-59.5	-19.5
38	ASN	PHI	-81.9	-41.9
39	LYS	PSI	-38.9	1.1
40	ASP	PHI	-105.7	-65.7
40	ASP	PSI	-29.6	10.4
41	TRP	PHI	-123.6	-67.1
41	TRP	PSI	112.2	159.1

42	TRP	PHI	-144.3	-104.3
42	TRP	PSI	114.3	175.6
43	LYS	PHI	-138.7	-62.6
43	LYS	PSI	103.5	151
44	VAL	PHI	-146.1	-94.4
44	VAL	PSI	112.9	178.5
50	GLN	PHI	-162.6	-88.7
50	GLN	PSI	132.5	172.5
51	GLY	PHI	153.3	193.3
51	GLY	PSI	-192.9	-152.9
52	PHE	PHI	-119.7	-67
52	PHE	PSI	116.3	163.4
53	VAL	PHI	-157.6	-104
53	VAL	PSI	124.7	175.2
54	PRO	PSI	108.5	148.5
55	ALA	PHI	-82.5	-42.5
55	ALA	PSI	-51.7	-11.7
56	ALA	PHI	-87.5	-47.5
56	ALA	PSI	-39.1	3.8
59	LYS	PHI	-149.6	-94.6
59	LYS	PSI	107.6	172.9
60	LYS	PHI	-99.5	-50.9
60	LYS	PSI	108.3	148.3
61	LEU	PHI	-104	-50.2
61	LEU	PSI	115.2	155.2

- Simultaneous multi-curve TREDOR fitting starting with Equation 1. This result can be extended[1] to a set of n_i equations, which is used to simultaneously fit the buildup curves of the individual carbon spins coupled to N_1.

$$n_i \begin{cases} V_{11}(t_m ix) = \Lambda_1(1-[J_0(\sqrt{2}D_{11}t_{mix})]^2)\prod_{k=2}^{n_i}(1+[J_0\sqrt{2}D_{1k}t_{mix}]^2) \\ V_{12}(t_m ix) = \Lambda_1(1-[J_0(\sqrt{2}D_{12}t_{mix})]^2)\prod_{k=1\neq 2}^{n_i}(1+[J_0\sqrt{2}D_{1k}t_{mix}]^2) \\ \ldots \\ V_{1i}(t_m ix) = \Lambda_1(1-[J_0(\sqrt{2}D_{1i}t_{mix})]^2)\prod_{k=1\neq i}^{n_i}(1+[J_0\sqrt{2}D_{1k}t_{mix}]^2) \end{cases} \quad (1)$$

Where Λ_1 is given as:

$$\Lambda_1 = \frac{1}{2^{n_i}}V_1(0)\lambda_1 exp(-\Gamma_1 t_{mix}) \quad (2)$$

The Γ_1 gives the coherence decay rate of spin coherence, which can be modeled as a single exponential. λ_1 is an amplitude scaling factor, which is typically fit freely since the starting signal is not recorded in a TEDOR measurement. So in a standard TEDOR fitting, to extract the dipolar couplings, one needs to fit the overall decay rate and an arbitrary scaling factor which are irrelevant to the parameter of concern. This consequently puts more demand on the data density, something that might be unachievable especially for samples with low sensitivity or short coherence times. In the pseudo-4D TREDOR experiment, we address this problem by recording the intensity of the untransferred part of the magnetization, so that the ratio $\zeta_{1i}(t_{mix})$ can be formed between transferred and total magnetization

$$\zeta_{1i}(t_{mix}) = \frac{V_{1i}(t_{mix})}{V_1(t_{mix}) + \sum_{k=1}^{n_i} V_{1k}(t_{mix})} \quad (3)$$

$$= \frac{V_{1i}(t_{mix})}{V_{total}(t_{mix})} \quad (4)$$

Where $V_1(t_{mix})$ is the intensity of the untransferred nitrogen signal, and the $V_{total}(t_{mix})$ is the total signal at a certain mixing time. The untransferred signal $V_1(t_{mix})$ appears with the same scaling and typically also the same decay parameter, and hence the total signal also follows a single exponential decay of the original signal intensity.

$$V_{total}(t_{mix}) = V_1(0)exp(-\Gamma_1 t_{mix}) \tag{5}$$

Normalization by the total signal results in a coherence decay-free TEDOR curve, for which the parameters λ_1 and $V_1(0)$ no longer appear. Combining Equation 1 and Equation 3, it is straightforward to show that we can fit the simultaneous buildup curve of several ^{13}C spins coupled to the same N_1 as the following set of equations:

$$n_i \begin{cases} \zeta_{11}(t_{mix}) = \frac{1}{2^{n_i}}(1 - [J_0(\sqrt{2}D_{11}t_{mix})]^2)\prod_{k=2}^{n_i}(1 + [J_0\sqrt{2}D_{1k}t_{mix}]^2) \\ \zeta_{12}(t_{mix}) = \frac{1}{2^{n_i}}(1 - [J_0(\sqrt{2}D_{12}t_{mix})]^2)\prod_{k=1\neq 2}^{n_i}(1 + [J_0\sqrt{2}D_{1k}t_{mix}]^2) \\ \ldots \\ \zeta_{1i}(t_{mix}) = \frac{1}{2^{n_i}}(1 - [J_0(\sqrt{2}D_{1i}t_{mix})]^2)\prod_{k=1\neq i}^{n_i}(1 + [J_0\sqrt{2}D_{1k}t_{mix}]^2) \end{cases} \tag{6}$$

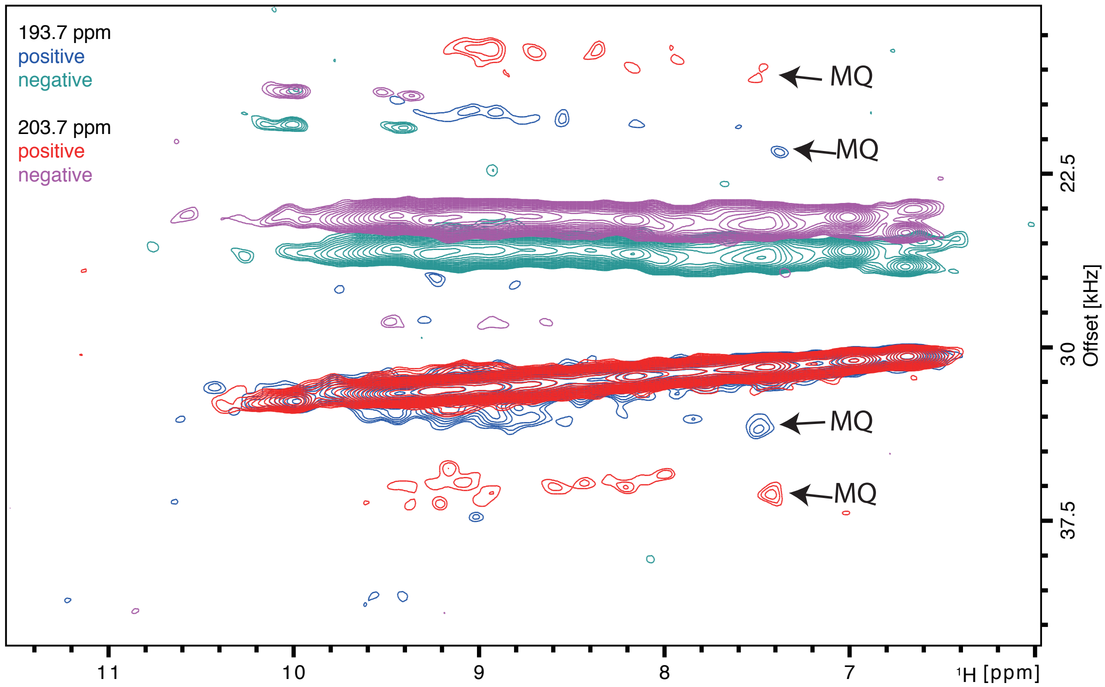

Figure S2. Comparison of positions of multiple quantum artifacts in pseudo-3D H-CO TREDOR. With a shift of the offset from 193.7 ppm to 203.7 ppm, the artifacts changed chemical shifts on the H-CO dimension each by 20 ppm, confirming the major artifacts left are only the leftover double quantum terms but not zero quantum terms. When the offset is placed at 203.7 ppm, the artifacts are placed away from the signal of interest enough for quantitative analysis.

Table S3. CO T2 rho in SH3 in ms with different hard pulse power in kHz and offsets in ppm

Power \ Offset	53 ppm	100 ppm
85 kHz	11.1 ms	64.7 ms
100 kHz	10.9 ms	60.4 ms

Table S4. CA T2 rho in SH3 in ms with different hard pulse power in kHz and offsets in ppm

Power \ Offset	53 ppm	100 ppm
85 kHz	41.0 ms	41.1 ms
100 kHz	47.5 ms	48.5 ms

References

(1) Jaroniec, C. P.; Filip, C.; Griffin, R. G. 3D TEDOR NMR experiments for the simultaneous measurement of multiple carbon-nitrogen distances in uniformly 13C,15N-labeled solids. *J. Am. Chem. Soc.* **2002**, *124*, 10728–10742.